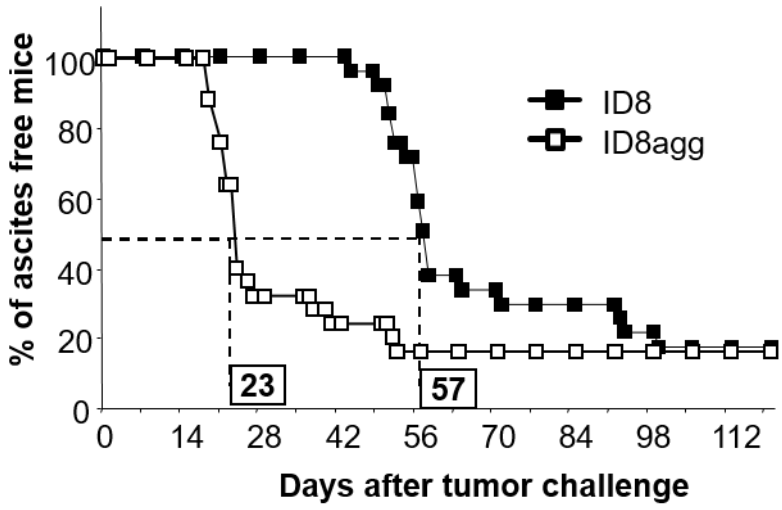

Suppl. Fig. 1. Aggressive variant of ID8 murine ovarian cancer. We generated an aggressive ID8 line, ID8agg, by serial passage through WT hosts. Numbers in boxes indicate median cohort time to ascites development.

Supplemental Figure 1

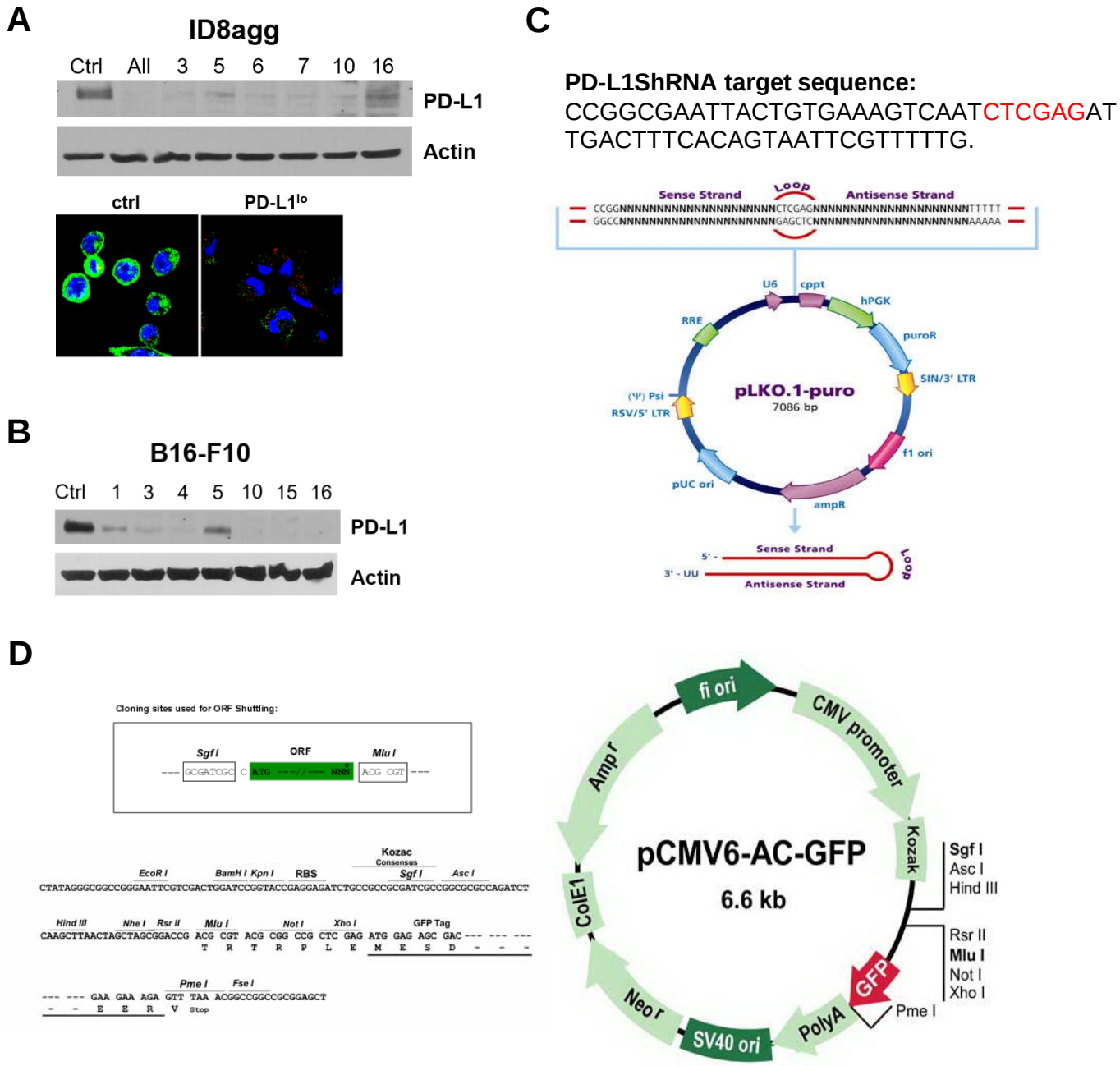

Suppl. Fig. 2. Genetic knock down of PD-L1 in ID8agg ovarian cancer and B16 melanoma cells using shRNA. We used plasmids stably expressing shRNA to reduce basal and PD-L1 expression (PD-L1^{lo}) in ID8agg (**A**) and B16 (**B**) cells, and a constitutively active vector to increase PD-L1 expression in B16 (PD-L1^{hi}, not shown). Confocal microscopy in **A** shows PD-L1 (green) and LC3 (red) in ID8agg. **C.** Stable PD-L1 knockdown in B16 and ID8agg lines was generated using lentivirus transduction particles containing validated PD-L1 shRNA (Sigma, TRCN0000068001) against murine *Pdcd1lg1* in pLKO.1-puro vector using puromycin selection per manufacturer's protocol **D.** The PD-L1-overexpressing (PD-L1^{hi}) B16 polyclonal line was generated by transfection of pCMV6-PD-L1-GFP plasmid (OriGene, MG203953) using Turbofect (ThermoFisher) per the manufacturer's protocol.

Supplemental Figure 2

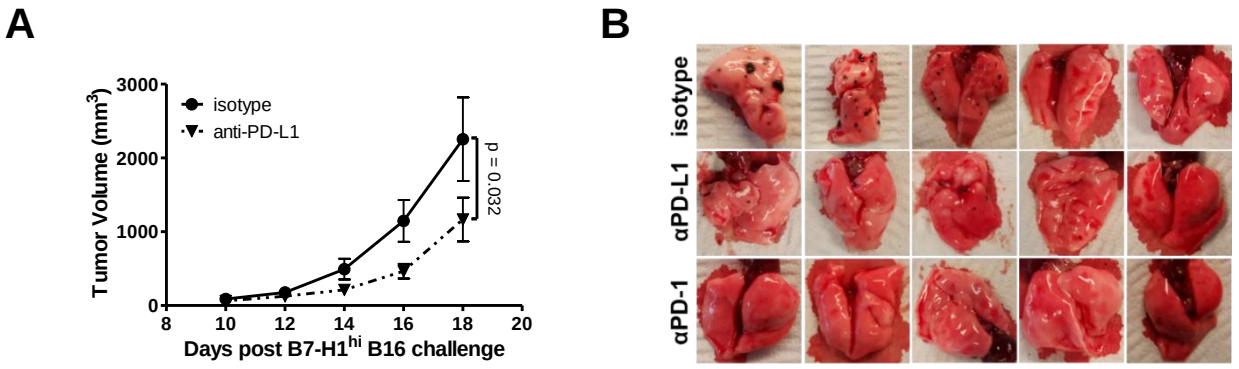

Suppl. Fig. 3. αPD-L1 reduces tumor growth and metastatic spread in NSG mice. **A.** NSG mice challenged subcutaneously with PD-L1^{hi} B16 cells and treated with αPD-L1 200 µg every other day starting one day following challenge. p-value, two-way ANOVA. **B.** Photos of representative lungs showing primary B16 metastases (black) from NSG mice challenged subcutaneously with parental B16 and sacrificed on day 18. αPD-L1 or αPD-1 or respective isotype controls given as in panels for **Fig. 2 B,C.**

Supplemental Figure 3

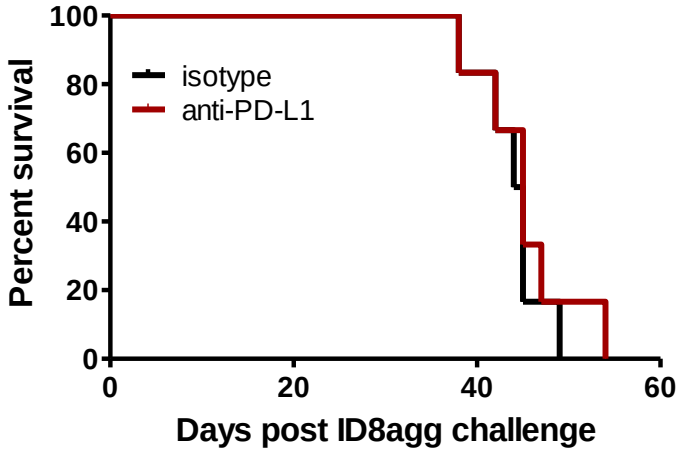

Suppl. Fig. 4. αPD-L1 immunotherapy fails to treat ID8agg in wild-type mice. WT mice were challenged with ID8agg cells and treated with anti-PD-L1 (100 µg/mouse) every 5 days starting day 7 following ID8agg challenge. PD-L1 KO mice were challenged with either control (**B**) or PD-L1^{lo} (**C**) B16 cells and treated with anti-PD-L1 (100 µg/mouse) every 5 days starting day 7 following B16 challenge.

Supplemental Figure 4

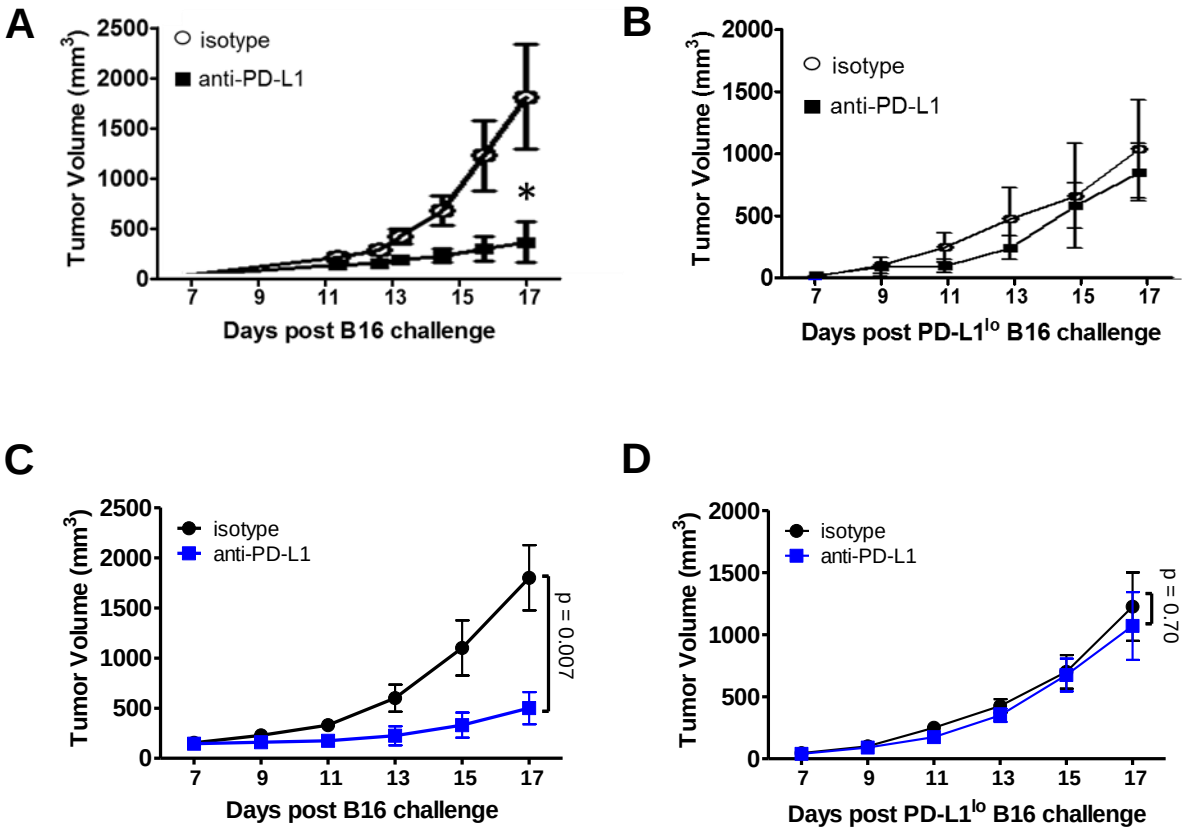

Suppl. Fig. 5. Tumor PD-L1 is necessary and sufficient for αPD-L1 treatment effects. WT mice were challenged with either control (**A**) or PD-L1^{lo} (**B**) B16 cells and treated with anti-PD-L1 (100 µg/mouse) every 5 days starting day 7 following B16 challenge. PD-L1 KO mice were challenged with either control (**C**) or PD-L1^{lo} (**D**) B16 cells and treated as in **A,B.**

Supplemental Figure 5

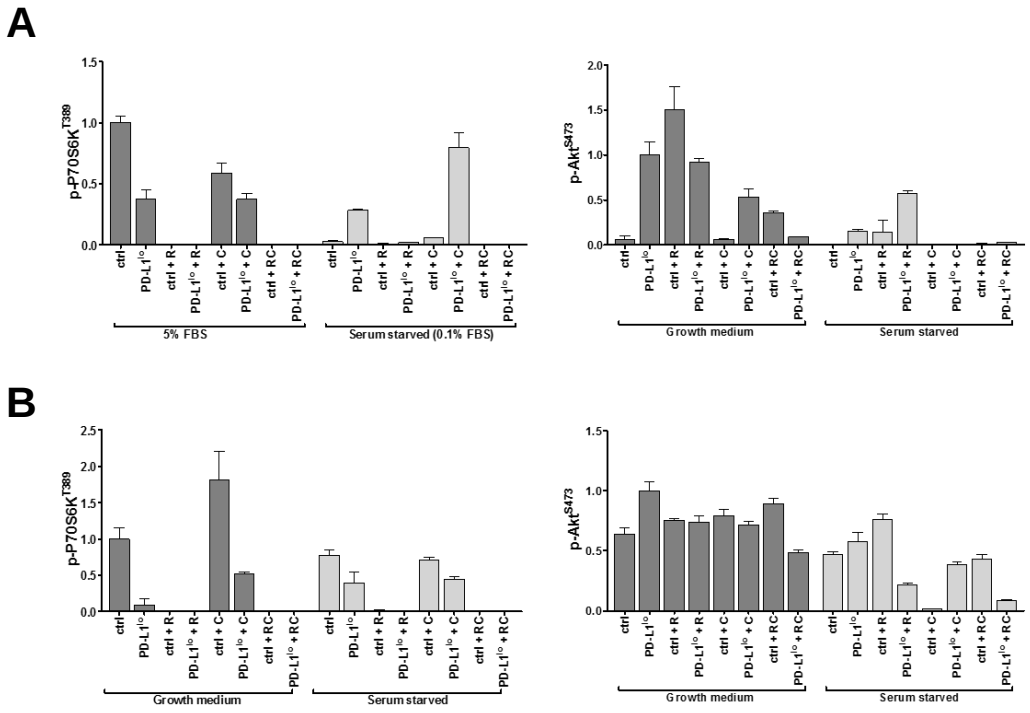

Suppl. Fig. 6. P70S6K^{T389} and Akt^{S478} signaling in ID8agg ovarian cancer and B16 melanoma cells under distinct conditions. Summary data of Western blots for P70S6K^{T389} and Akt^{S473} as ratios of phospho-protein/total protein under basal or serum starved (24 h) conditions for ID8agg (**A**) and B16 (**B**) cells and pre-treatment with rapamycin (R) for 16 h, chloroquine (C) for 6 h or both (R+C). Means from 3 independent blots shown.

Supplemental Figure 6

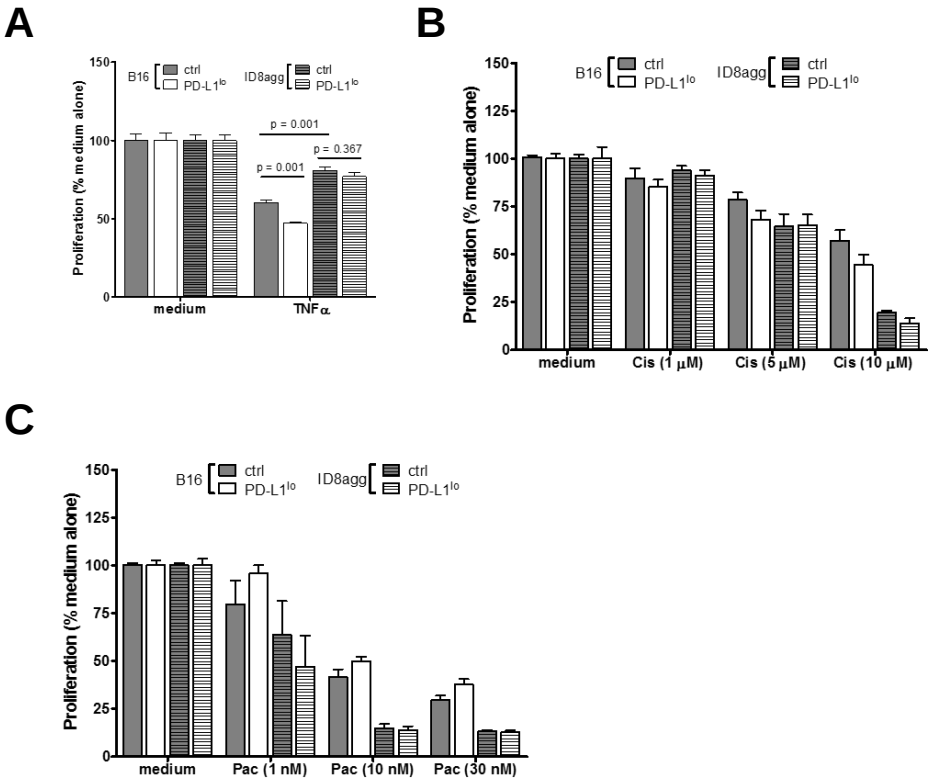

Suppl. Fig. 7. Effect of tumor cell PD-L1 expression on proliferation sensitivity to TNFα and chemotherapy. A. Proliferation *in vitro* of B16 cells ± TNFα (10 ng/mL) determined by MTT versus control (ctrl, set at 100%). p-value, unpaired *t* test. B. Proliferation *in vitro* of B16 cells ± cisplatin (**B**) or paclitaxel (**C**) at indicated dose, as in **A.**

Supplemental Figure 7